JOURNAL OF GUIDANCE, CONTROL, AND DYNAMICS
Vol. 25, No. 3, May–June 2002

Epicyclic Motion of Satellites Under Rotating Potential

Yoshikazu Hashida* and Philip L. Palmer†
University of Surrey, Guildford, England GU2 7XH, United Kingdom

Further to our work on the epicyclic description of perturbed orbits under axisymmetric potential, we present the extended analysis focusing on the tesseral harmonic potential. We restrict the problem to a near-circular orbit of which eccentricity is assumed to be of order J_2—Earth's second zonal harmonic—and introduce the analytical formulation of first-order perturbed epicycle orbit up to an arbitrary degree and order of tesseral harmonics. Some periodic terms of interest as a result of tesseral terms are discussed. Explicit coefficients for these periodic terms are also given for second and third degrees. We have shown that the amplitude of the fourth-degree tesseral periodic perturbations can become larger than that of the second-order tesserals for some specific orbits and the conditions for this are addressed. We also present simulation results to establish the accuracy of our epicycle modeling by comparing with numerically integrated orbits, and we obtain only subkilometer positional error after 5000 orbits propagation for a low-Earth near-circular orbit.

Introduction

IN 1959 Kozai[1] and Brouwer[2] introduced analytic solutions of the perturbed orbital elements of a satellite moving in as axisymmetric potential. Since then, there has been an extensive body of literature studying the motion of satellites in axisymmetric potentials. Merson[3] evaluated the perturbation of an orbit caused by several low-degree zonal harmonics. Cook[4] summarized the nature of long periodic variations for particularly near-circular orbit up to an arbitrary odd zonal harmonic degree. Recently, by focusing on only near-circular orbits whose eccentricities are assumed to be $\mathcal{O}(J_2)$ Hashida and Palmer[5] reviewed this problem and reformulated the perturbative motion of satellites in terms of a new epicyclic description, which brings mathematical simplicity of the formulations and also provides a simple geometric interpretation of the description of the orbit.

In 1960 Musen[6] presented a method for the determination of tesseral/sectoral (hereinafter simply tesseral) harmonics in the gravitational field, with the availability of more accurate data and extended over longer intervals of time. Cook,[7] in 1963, published complete descriptions of long-periodic variations caused by tesseral harmonics up to the fourth degree without any assumptions on inclination and eccentricity. Kaula[8] derived generalized expressions for first-order perturbations for any term in the potential. He converted the spherical harmonic potential in terms of the classical Keplerian elements by introducing the inclination and eccentricity functions and solved the problem through Lagrange's planetary equations.

In this paper we review the problem of tesseral harmonics for near-circular orbits by using the epicycle description; therefore, this article represents an extension of our work on satellite epicyclic motion under a zonal potential.[5] We have shown the first-order tesseral perturbations up to an arbitrary degree by the use of Kaula's inclination functions.[8] Our simple formulation of the perturbed orbit is useful not only for analytical approaches to mission analysis, but also for the design of an onboard orbit estimator. An orbit estimator using analytical solutions of perturbed orbits, in spite of its moderate accuracy, might be preferable especially for micro- or even nano-satellites where the processing resources might be limited.

We briefly review the description of epicycle orbits around a spherical Earth and interpret these basic descriptive equations. We then derive the linearized equations of motion in the variables we have chosen. We provide first-order analytic solutions to these equations for each term in the tesseral harmonic expansion and discuss some terms of interest. Finally, we show comparisons of these analytic formulas with accurate numerical simulations of satellite orbits.

Received 18 January 2001; revision received 26 September 2001; accepted for publication 8 October 2001.

*Engineer, Surrey Space Centre, Surrey Satellite Technology Ltd.
†Reader, Surrey Space Centre.

Keplerian Epicycle

We begin by reviewing briefly the epicycle motion of satellites in low-eccentricity orbits about a spherical Earth.[5] The Keplerian equations of motion are

$$\ddot{r} - r\dot{\lambda}^2 = -\frac{\mu}{r^2}, \qquad \frac{\mathrm{d}}{\mathrm{d}t}(r^2\dot{\lambda}) = 0 \tag{1}$$

described in some polar coordinates (r, λ), where μ is the gravitational parameter. For circular orbits we can find a solution to Eqs. (1) in which $r = a$ and $\dot{\lambda} = n_0$, where both a and n_0 are constants that satisfy $a^3 {n_0}^2 = \mu$. We are interested in the motions of satellites in very low-eccentricity orbits, which can be found by perturbing the preceding solution. For this, let $r = a + s$ and $\dot{\lambda} = n_0 + \dot{\epsilon}$. Ignoring second-order terms in these small corrections, we have shown Eqs. (1) are linearized by

$$\frac{\ddot{s}}{an_0^2} + \frac{s}{a} = 2\left(\frac{2s}{a} + \frac{\dot{\epsilon}}{n_0}\right), \qquad \frac{\mathrm{d}}{\mathrm{d}t}\left(\frac{2s}{a} + \frac{\dot{\epsilon}}{n_0}\right) = 0 \tag{2}$$

The orbital energy is also linearized by

$$\mathcal{E} = -(\mu/2a)[1 - 2(2s/a + \dot{\epsilon}/n_0)] \tag{3}$$

Therefore through Eq. (3), by choosing the mean radius a as the radius of a circular orbit of the same orbital energy, the second of Eq. (2) can be integrated by

$$2s/a + \dot{\epsilon}/n_0 = 0 \tag{4}$$

We formulate the epicycle description of Keplerian orbits by solving the first of Eqs. (2) and Eq. (4) and can easily expand to three-dimensional motion because the inclination I and ascending node Ω stay constant:

$$r = a - A\cos(\alpha - \alpha_P), \qquad I = I_0, \qquad \Omega = \Omega_0$$

$$\lambda = \alpha + (2A/a)[\sin(\alpha - \alpha_P) + \sin\alpha_P] \tag{5}$$

The angle α is defined through the mean motion n_0 by $n_0 t$ and measured from the ascending node, called epicycle phase. Two parameters A and α_P are integration constants, called epicycle amplitude and epicycle phase at the perigee passage. We are assuming $\mathcal{O}(A/a) \approx \mathcal{O}(J_2)$ throughout this paper. We also show that the argument of perigee ω is related to α_P through

$$\omega = \alpha_P + (2A/a)\sin\alpha_P \tag{6}$$

We are describing the position of a Keplerian orbit using four coordinates of (r, I, Ω, λ). Two coordinates I and Ω determine the orientation of the orbital plane in three-dimensional space, and another two coordinates, r and λ, represent the position of a satellite in this orbital plane by the epicyclic description.

One might notice that we do not have a secular term in the azimuthal λ solution in Eqs. (5) because of the choice of our semimajor axis. This choice, however, can always be performed if we consider only one satellite. This implies that a major orbit control problem can arise in order to eliminate the relative secular term if a cluster of satellites, such as a satellite constellation or formation flying, is considered.

Linearized Equations of Motion

In this section we derive the linearized equations of motion describing the motion of a satellite in three dimensions using the four-coordinates representation developed in the preceding section.

Equations of Motion in New Variables

Starting from spherical polar coordinates (r, θ, φ), the equations of motion under a rotating potential are

$$\ddot{r} - r(\dot{\theta}^2 + \dot{\varphi}^2 \sin^2\theta) = -\frac{\mu}{r^2} - \frac{\partial V}{\partial r}$$

$$\frac{\mathrm{d}}{\mathrm{d}t}(r^2\dot{\theta}) - r^2\dot{\varphi}^2 \sin\theta\cos\theta = -\frac{\partial V}{\partial \theta}$$

$$\frac{\mathrm{d}}{\mathrm{d}t}(r^2\dot{\varphi}\sin^2\theta) = -\frac{\partial V}{\partial \varphi} \tag{7}$$

We relate the conventional notation of C_{nm} and S_{nm} to J_{nm} by

$$C_{nm} = J_{nm}\cos m\psi_{nm}, \qquad S_{nm} = J_{nm}\sin m\psi_{nm} \tag{8}$$

ψ_{nm} is not uniquely determined because of unknown factors, which are multiples of $2\pi/m$; however, we shall take the smallest positive value for ψ_{nm}.[7] The angle ψ, which is geographic longitude, is related to φ by

$$\psi = \varphi - \theta_g \tag{9}$$

and θ_g is Greenwich sidereal time expressed as an angle. Then the potential V caused by the l-deg zonal and the n-deg m-order tesseral contribution in Eq. (7) is given by

$$V = (\mu/r)J_l(R/r)^l P_l(\cos\theta) - (\mu/r)J_{nm}(R/r)^n P_n^m(\cos\theta)\cos m(\psi - \psi_{nm}) \tag{10}$$

where we have assumed $m \neq 0$ throughout this manuscript. The notation of R is the Earth's mean equatorial radius.

We can relate the position of the satellite (θ, φ) to the orbital parameters (I, Ω, λ) such that

$$\sin\theta\cos(\varphi - \Omega) = \cos\lambda, \qquad \sin\theta\sin(\varphi - \Omega) = \cos I\sin\lambda$$

$$\cos\theta = \sin I\sin\lambda \tag{11}$$

We also have the following useful equalities[5]:

$$\dot{\varphi}\sin^2\theta = \dot{\nu}\cos I, \qquad \dot{\theta}\sin\theta = -\dot{\nu}\sin I\cos\lambda$$

$$\dot{\theta}^2 + \dot{\varphi}^2\sin^2\theta = \dot{\nu}^2, \qquad \dot{I}\sin\lambda = \dot{\Omega}\sin I\cos\lambda$$

$$\dot{\nu} = \dot{\lambda} + \dot{\Omega}\cos I \tag{12}$$

where ν is the true anomaly. By differentiating the first and second of Eqs. (11), we can show that

$$\frac{\partial}{\partial\theta} = -\frac{\cos I}{\sin\theta\sin\lambda}\frac{\partial}{\partial I} - \frac{\sin I\cos\lambda}{\sin\theta}\frac{\partial}{\partial\lambda}$$

$$\frac{\partial}{\partial\phi} = -\frac{\sin I\cos\lambda}{\sin\lambda}\frac{\partial}{\partial I} + \cos I\frac{\partial}{\partial\lambda} \tag{13}$$

where $\phi = \varphi - \Omega = \psi + \theta_g - \Omega$.

By introducing $h_z = r^2\dot{\nu}\cos I$, which is the z component of angular momentum, the third of Eqs. (7) is

$$\dot{h_z} = -\frac{\partial V}{\partial\varphi} \tag{14}$$

If we multiply through the second of Eqs. (7) by $\sin\theta$, we can write it in the form:

$$\frac{\mathrm{d}}{\mathrm{d}t}(r^2\dot{\nu}\sin I\cos\lambda) + r^2\dot{\nu}^2\sin I\sin\lambda = \sin\theta\frac{\partial V}{\partial\theta} \tag{15}$$

Using Eqs. (12) and (14), we can write this equation as

$$h_z\dot{I}\sin^2\theta = \cos^2 I\cos\lambda\left(\sin\theta\frac{\partial V}{\partial\theta} + \tan I\cos\lambda\frac{\partial V}{\partial\varphi}\right) \tag{16}$$

The ascending node equation is then obtained by the fourth of Eqs. (12) through Eq. (16), and the radial equation, the first of Eqs. (7), is given by

$$\ddot{r} - r\dot{\nu}^2 = -\frac{\mu}{r^2} - \frac{\partial V}{\partial r} \tag{17}$$

Kaula[8] and Palmer[9] have introduced an inclination function $F_{nmp}(I)$ through the relations:

$$P_n^m(\cos\theta)\cos m\phi = \sum_{p=0}^{n} F_{nmp}(I)\cos(n-2p)\lambda$$

$$P_n^m(\cos\theta)\sin m\phi = \sum_{p=0}^{n} F_{nmp}(I)\sin(n-2p)\lambda \tag{18}$$

if $(n-m)$ is even, and

$$P_n^m(\cos\theta)\cos m\phi = \sum_{p=0}^{n} F_{nmp}(I)\sin(n-2p)\lambda$$

$$P_n^m(\cos\theta)\sin m\phi = -\sum_{p=0}^{n} F_{nmp}(I)\cos(n-2p)\lambda \tag{19}$$

if $(n-m)$ is odd. The inclination function $F_{nmp}(I)$ is defined by

$$F_{nmp}(I) = \sum_{t=0}^{\min(p,k)} \frac{(2n-2t)!}{2^{2n-2t}t!(n-t)!(n-m-2t)!} \times \sin^{n-m-2t}I\sum_{s=0}^{m}\binom{m}{s}\cos^s I\sum_c(-1)^{c-k} \times \binom{n-m-2t+s}{c}\binom{m-s}{p-t-c} \tag{20}$$

where k is the integer part of $(n-m)/2$ and c is summed for all values for which the coefficients are not equal to zero.

For convenience, we shall define the following functions:

$$C_{nmp}(\lambda, \Omega, \theta_g) = \left\{\begin{matrix}\cos\\ \sin\end{matrix}\right\}_{(n-m)\text{ odd}}^{(n-m)\text{ even}} [(n-2p)\lambda + m(\Omega - \theta_g - \psi_{nm})]$$

$$S_{nmp}(\lambda, \Omega, \theta_g) = \left\{\begin{matrix}\sin\\ -\cos\end{matrix}\right\}_{(n-m)\text{ odd}}^{(n-m)\text{ even}} [(n-2p)\lambda + m(\Omega - \theta_g - \psi_{nm})] \tag{21}$$

Using Eqs. (18) or (19), the potential Eq. (10) is rearranged by

$$V = \frac{\mu}{r}J_l\left(\frac{R}{r}\right)^l P_l(\sin I\sin\lambda) - \frac{\mu}{r}J_{nm}\left(\frac{R}{r}\right)^n \times \sum_{p=0}^{n} F_{nmp}(I)C_{nmp}(\lambda, \Omega, \theta_g) \tag{22}$$

By computing $\partial V/\partial\phi$, $\partial V/\partial I$, and $\partial V/\partial\lambda$, the second of Eqs. (13) results in the following equality:

$$[m-(n-2p)\cos I]F_{nmp}(I)S_{nmp}(\lambda,\Omega,\theta_g)\sin\lambda = \sin I F'_{nmp}(I)C_{nmp}(\lambda,\Omega,\theta_g)\cos\lambda \tag{23}$$

where the notation of $F'_{nmp}(I)=\mathrm{d}F_{nmp}(I)/\mathrm{d}I$ is introduced.

The angular momentum equation of Eq. (14) becomes

$$\dot{h}_z = -m\frac{\mu}{r}J_{nm}\left(\frac{R}{r}\right)^n\sum_{p=0}^{n}F_{nmp}(I)S_{nmp}(\lambda,\Omega,\theta_g) \tag{24}$$

The inclination equation (16) is arranged by

$$h_z\dot{I} = -\frac{\mu}{r}J_l\left(\frac{R}{r}\right)^l\cos^2 I\cos\lambda\frac{\mathrm{d}P_l(\sin I\sin\lambda)}{\mathrm{d}(\sin I\sin\lambda)} + \frac{\mu}{r}J_{nm}\left(\frac{R}{r}\right)^n \times\cot I\sum_{p=0}^{n}[m-(n-2p)\cos I]F_{nmp}(I)S_{nmp}(\lambda,\Omega,\theta_g) \tag{25}$$

Then the ascending node equation is found through the fourth of Eqs. (12) by

$$h_z\dot{\Omega} = -\frac{\mu}{r}J_l\left(\frac{R}{r}\right)^l\cos I\cot I\sin\lambda\frac{\mathrm{d}P_l(\sin I\sin\lambda)}{\mathrm{d}(\sin I\sin\lambda)} + \frac{\mu}{r}J_{nm}\left(\frac{R}{r}\right)^n\cot I\sum_{p=0}^{n}F'_{nmp}(I)C_{nmp}(\lambda,\Omega,\theta_g) \tag{26}$$

Note that Eq. (23) is used to obtain both inclination and ascending node equations. The radial equation (17) is given by

$$\ddot{r}-r\dot{\nu}^2 = -\frac{\mu}{r^2}+(l+1)\frac{\mu}{r^2}J_l\left(\frac{R}{r}\right)^l P_l(\sin I\sin\lambda) - (n+1)\frac{\mu}{r^2}J_{nm}\left(\frac{R}{r}\right)^n\sum_{p=0}^{n}F_{nmp}(I)C_{nmp}(\lambda,\Omega,\theta_g) \tag{27}$$

Jacobi Constant of Motion

Unlike the motion under axisymmetric potential, both the orbital energy and the z component of the angular momentum vector are no longer conserved. However, we can show the constant of motion by introducing a rotating coordinate, which is known as the Jacobi constant. The Jacobi constant $\mathcal{C}$ is given by

$$\tfrac{1}{2}\left[\dot{r}^2+(r\dot{\theta})^2+r^2\left(\dot{\psi}^2-\omega_\oplus^2\right)\sin^2\theta\right]-\mu/r+V=\mathcal{C} \tag{28}$$

where we introduce the notation of $\omega_\oplus=\dot{\theta}_g$, which is the Earth's sidereal rotation rate. The derivation of Jacobi constant Eq. (28) is shown in the Appendix of this paper. Reverting back the coordinate ψ to φ by $\dot{\psi}=\dot{\varphi}-\omega_\oplus$ and using the first of Eqs. (12), we find the Jacobi constant:

$$\mathcal{C}=\mathcal{E}-\omega_\oplus r^2\dot{\nu}\cos I=\mathcal{E}-\omega_\oplus h_z \tag{29}$$

where the notation $\mathcal{E}$ represents the orbital energy.

First-Order Linearized Equations

We seek solutions to the preceding equations (24–26) in the neighborhood of circular orbits. Let us define I_0 and Ω_0 as instantaneous (or osculating) inclination and right ascension of the ascending node at an epoch when the instantaneous argument of latitude reaches zero (or at an initial ascending node). We shall take into account J_{2l} even-degree zonal terms to linearize the J_{nm} tesseral equations because even-zonal harmonics introduce secular perturbations on our argument of latitude and right ascension of the ascending node. The dominant $J_2(l=1)$ harmonic will be the most practical term of interest.

Let us represent our coordinates by

$$r=a+s_{2l}+s_{nm},\qquad I=I_0+\iota_{2l}+\iota_{nm}$$
$$\Omega=\Omega_0+o_{2l}+o_{nm},\qquad \lambda=\alpha+\epsilon_{2l}+\epsilon_{nm} \tag{30}$$

where the definition of a, the mean semimajor axis, shall be given in a later section. The α angle, mean argument of latitude or epicycle phase, is then defined by n_0t through $a^3n_0^2=\mu$. s_{2l}, ι_{2l}, o_{2l}, and ϵ_{2l} are small correction terms from the J_{2l} potential including the Keplerian epicycle terms[5]:

$$s_{2l}=a\varrho-A\cos(\alpha-\alpha_P)+\sum_{k=1}^{l}\Delta r_{2l}^k\cos 2k\alpha$$
$$\iota_{2l}=\sum_{k=1}^{l}\Delta I_{2l}^k(1-\cos 2k\alpha),\qquad o_{2l}=\vartheta\alpha+\sum_{k=1}^{l}\Delta\Omega_{2l}^k\sin 2k\alpha$$
$$\epsilon_{2l}=\kappa\alpha+(2A/a)[\sin(\alpha-\alpha_P)+\sin\alpha_P]+\sum_{k=1}^{l}\Delta\lambda_{2l}^k\sin 2k\alpha \tag{31}$$

and explicit coefficients in Eq. (31) are introduced in the Appendix. Note that ϑ and κ are secular perturbation terms. We have shown that the zonal solutions satisfy following equality[5]:

$$\delta_{2l}=\frac{2s_{2l}}{a}-\iota_{2l}\tan I_0+\frac{\mathrm{d}\epsilon_{2l}}{\mathrm{d}\alpha}+\frac{\mathrm{d}o_{2l}}{\mathrm{d}\alpha}\cos I_0=-J_{2l}\left(\frac{R}{a}\right)^{2l}P_{2l}(0) \tag{32}$$

s_{nm}, ι_{nm}, o_{nm}, and ϵ_{nm} are caused by J_{nm} tesseral potential, which we are going to evaluate through this paper. We also describe sidereal time θ_g in terms of epicycle phase α, which is a dimensionless time, such that

$$\theta_g=\theta_0+\omega_\oplus t=\theta_0+\omega_e\alpha \tag{33}$$

where θ_0 is the sidereal time at $t=0$; hence, $\alpha=0$. Note that ω_e is the sidereal Earth rotation rate normalized by the satellite mean motion n_0, e.g., $\omega_e=\omega_\oplus/n_0$.

Let us introduce the following abbreviations:

$$C_{nmp}(\alpha):=C_{nmp}[(1+\kappa)\alpha,\Omega_0+\vartheta\alpha,\theta_0+\omega_e\alpha] = \begin{Bmatrix}\cos\\ \sin\end{Bmatrix}_{(n-m)\,\mathrm{odd}}^{(n-m)\,\mathrm{even}}[\tau_{nmp}\alpha+m(\Omega_0-\theta_0-\psi_{nm})]$$
$$S_{nmp}(\alpha):=S_{nmp}[(1+\kappa)\alpha,\Omega_0+\vartheta\alpha,\theta_0+\omega_e\alpha] = \begin{Bmatrix}\sin\\ -\cos\end{Bmatrix}_{(n-m)\,\mathrm{odd}}^{(n-m)\,\mathrm{even}}[\tau_{nmp}\alpha+m(\Omega_0-\theta_0-\psi_{nm})] \tag{34}$$

where τ_{nmp} is defined by

$$\tau_{nmp}=(n-2p)(1+\kappa)+m(\vartheta-\omega_e) \tag{35}$$

Then for the first-order approximation C_{nmp} and S_{nmp} functions with J_{nm} coefficients can be regarded as a function of epicycle phase α because we have

$$\begin{Bmatrix}C_{nmp}(\lambda,\Omega,\theta_g)\\ S_{nmp}(\lambda,\Omega,\theta_g)\end{Bmatrix}\approx\begin{Bmatrix}C_{nmp}(\alpha)\\ S_{nmp}(\alpha)\end{Bmatrix}+\begin{Bmatrix}-S_{nmp}(\alpha)\\ C_{nmp}(\alpha)\end{Bmatrix}\Delta\alpha_{nmp} \tag{36}$$

where

$$\Delta\alpha_{nmp}=(n-2p)(\epsilon_{2l}-\kappa\alpha+\epsilon_{nm})+m(o_{2l}-\vartheta\alpha+o_{nm}) \tag{37}$$

and $\Delta\alpha_{nmp}$ is a periodic term of $\mathcal{O}(A/a, J_{2l}, J_{nm})$; therefore, we can ignore the second term of the right-hand side of Eq. (36).

Using the last of Eqs. (12) and substituting our representation of coordinates (30) to h_z, they can be linearized by

$$h_z=a^2n_0(1+\delta_{2l}+\delta_{nm})\cos I_0 \tag{38}$$

where

$$\delta_{nm}=\frac{2s_{nm}}{a}-\iota_{nm}\tan I_0+\frac{\mathrm{d}\epsilon_{nm}}{\mathrm{d}\alpha}+\frac{\mathrm{d}o_{nm}}{\mathrm{d}\alpha}\cos I_0 \tag{39}$$

Unlike for a zonal potential, δ_{nm} is no longer constant (δ_{2l} is a constant). Linearizing Eq. (24) gives

$$\frac{\mathrm{d}\delta_{nm}}{\mathrm{d}\alpha} = -mJ_{nm}\left(\frac{R}{a}\right)^n \sum_{p=0}^{n} \frac{F_{nmp}(I_0)}{\cos I_0} S_{nmp}(\alpha) \tag{40}$$

The inclination equation (25) and ascending node equation (26) are linearized by

$$\frac{\mathrm{d}\iota_{nm}}{\mathrm{d}\alpha} = J_{nm}\left(\frac{R}{a}\right)^n \sum_{p=0}^{n} \frac{[m-(n-2p)\cos I_0]F_{nmp}(I_0)}{\sin I_0} S_{nmp}(\alpha) \tag{41}$$

$$\frac{\mathrm{d}o_{nm}}{\mathrm{d}\alpha} = J_{nm}\left(\frac{R}{a}\right)^n \sum_{p=0}^{n} \frac{F'_{nmp}(I_0)}{\sin I_0} C_{nmp}(\alpha) \tag{42}$$

We also obtain the linearized radial equation such that

$$\frac{\mathrm{d}^2}{\mathrm{d}\alpha^2}\left(\frac{s_{nm}}{a}\right) + \frac{s_{nm}}{a} = 2\delta_{nm} + 2\iota_{nm}\tan I_0 - (n+1)J_{nm}\left(\frac{R}{a}\right)^n \sum_{p=0}^{n} F_{nmp}(I_0)C_{nmp}(\alpha) \tag{43}$$

Equations (40–43) represent the linearized equations of motion under the tesseral potential. All J_{2l} terms are canceled out for the given solutions of s_{2l}, ι_{2l}, o_{2l}, and ϵ_{2l}.

Solving Linearized Equations

In this section we shall derive first-order solutions to the linearized equations (40–43) obtained in the preceding section.

First-Order Solutions Caused by Tesseral Harmonics

By integrating Eq. (41), we obtain

$$\iota_{nm} = J_{nm}\left(\frac{R}{a}\right)^n \sum_{p=0}^{n} \frac{[(n-2p)\cos I_0 - m]F_{nmp}(I_0)}{\tau_{nmp}\sin I_0} \times [C_{nmp}(\alpha) - C_{nmp}(0)] \tag{44}$$

The ascending node perturbation is also solved by

$$o_{nm} = J_{nm}\left(\frac{R}{a}\right)^n \sum_{p=0}^{n} \frac{F'_{nmp}(I_0)}{\tau_{nmp}\sin I_0}[S_{nmp}(\alpha) - S_{nmp}(0)] \tag{45}$$

The angular momentum equation (40) is integrated to give

$$\delta_{nm} = mJ_{nm}\left(\frac{R}{a}\right)^n \sum_{p=0}^{n} \frac{F_{nmp}(I_0)}{\tau_{nmp}\cos I_0} C_{nmp}(\alpha) - \delta^0_{nm} \tag{46}$$

and δ^0_{nm} is some integration constant that needs to be determined. Notice that δ_{nm} is not necessarily zero at $t=0$ ($\alpha=0$). Substituting δ_{nm} and ι_{nm} solutions of Eqs. (44) and (46) into the radial equation (43) and ignoring the complimentary function (which is just the epicycle term already accounted for), we obtain the radial perturbation solution s_{nm} such that

$$\frac{s_{nm}}{a} = -2\left(\delta^0_{nm} + \iota^0_{nm}\tan I_0\right) - J_{nm}\left(\frac{R}{a}\right)^n \times \sum_{p=0}^{n} \frac{[(n+1)\tau_{nmp} - 2(n-2p)]F_{nmp}(I_0)}{\tau_{nmp}\left(1-\tau^2_{nmp}\right)} C_{nmp}(\alpha) \tag{47}$$

where the notation of ι^0_{nm} is introduced through Eq. (44) by

$$\iota^0_{nm} = J_{nm}\left(\frac{R}{a}\right)^n \sum_{p=0}^{n} \frac{[(n-2p)\cos I_0 - m]F_{nmp}(I_0)}{\tau_{nmp}\sin I_0} C_{nmp}(0) \tag{48}$$

When we substitute all of the solutions we have derived into Eq. (39), we can formulate the azimuthal equation by

$$\frac{\mathrm{d}\epsilon_{nm}}{\mathrm{d}\alpha} + \frac{\mathrm{d}o_{nm}}{\mathrm{d}\alpha}\cos I_0 = 3\left(\delta^0_{nm} + \iota^0_{nm}\tan I_0\right) + J_{nm}\left(\frac{R}{a}\right)^n \times \sum_{p=0}^{n}\left\{(n-2p) + \frac{2[(n+1)\tau_{nmp} - 2(n-2p)]}{1-\tau^2_{nmp}}\right\} \times \frac{F_{nmp}(I_0)}{\tau_{nmp}} C_{nmp}(\alpha) \tag{49}$$

The azimuthal equation (49) is integrated by

$$\epsilon_{nm} + o_{nm}\cos I_0 = 3\left(\delta^0_{nm} + \iota^0_{nm}\tan I_0\right)\alpha + J_{nm}\left(\frac{R}{a}\right)^n \times \sum_{p=0}^{n}\left\{(n-2p) + \frac{2[(n+1)\tau_{nmp} - 2(n-2p)]}{1-\tau^2_{nmp}}\right\} \times \frac{F_{nmp}(I_0)}{\tau^2_{nmp}}[S_{nmp}(\alpha) - S_{nmp}(0)] \tag{50}$$

All of our solutions introduced here meet a singularity when $\tau_{nmp} \approx 0$. This case is a resonance between the orbital frequency and the Earth's rotation frequency. Recalling the notation of ω_e, which is the dimensionless Earth's rotation rate normalized by the satellite epicycle frequency n_0, e.g., $\omega_e = \omega_\oplus/n_0$, then $\tau_{nmp} = 0$ yields

$$(n-2p)(1+\kappa)n_0 + m(\vartheta n_0 - \omega_\oplus) = 0 \tag{51}$$

which occurs if

$$n_0 = \frac{m\omega_\oplus}{(n-2p)(1+\kappa) + m\vartheta} \tag{52}$$

For the particular case of $(n-2p) = m$ for which $(n-m)$ must be even, Eq. (52) results in $n_0 \approx \omega_\oplus$. This shows that the epicycle frequency is approximately one rotation per one sidereal day, which is the case for a 24-hour orbit or geosynchronous orbit. Also if $n-2p = \pm 1$, then we have $n_0 \approx m\omega_\oplus$, making our solution unstable. This will happen if the satellite orbital period is an integer fraction of a day, for instance, 12, 8-hour orbits. In addition, both the radial and the azimuthal solutions have the $(1-\tau^2_{nmp})$ divisor, which introduces instabilities if $\tau_{nmp} \approx \pm 1$. Similarly $\tau_{nmp} = \pm 1$ are solved for n_0 by

$$n_0 = \frac{m\omega_\oplus}{(n-2p\mp 1) + (n-2p)\kappa + m\vartheta} \tag{53}$$

These solutions indicate that if $(n-2p\mp 1) = m$ for which $(n-m)$ must be odd, then they become $n_0 \approx \omega_\oplus$. Also Eq. (53) yields $n_0 \approx m\omega_\oplus$ when $n-2p = 2, 0$.

The detailed studies are made, for instance, by Blitzer et al.[10] for the geostationary orbit and by Gedeon[11] who showed libration periods for several circular resonant orbits including subsynchronous orbits such as 12-hour, 8-hour orbits.

Recently, through the analysis of the precise TOPEX/Poseidon orbit, the effect of near-resonant tesseral harmonic perturbations in semimajor axis is mentioned and the variations in semimajor axis due to the tesseral harmonic J_{nm} with n in the range of 13–19 and m with the values 12 and 13 are reported.[12] The overall resonance effects from tesseral harmonics are summarized by Vallado.[13] Some interesting tesseral solutions with $\tau_{nmp} = \mathcal{O}(m\omega_e)$ and $1-\tau^2_{nmp} = \mathcal{O}(m\omega_e)$ are investigated in a later section.

Definition of Semimajor Axis

We have to define the mean semimajor axis a found in Eq. (30) by which we have linearized the equations. When only a zonal potential is considered, we define the mean semimajor axis a in terms of the orbital energy, which is conserved.[5] However, if the tesseral potential is included, the orbital energy is no longer constant, so that we shall define a through the Jacobi constant $\mathcal{C}$.

Substituting our representation of coordinates (30) to the orbital energy $\mathcal{E}$ equation, the first-order approximation to $\mathcal{E}$ is obtained by

$$\mathcal{E} = -\frac{\mu}{2a} + \frac{\mu}{a}\left[\delta_{nm} + \iota_{nm}\tan I_0 - J_{nm}\left(\frac{R}{a}\right)^n \times \sum_{p=0}^{n} F_{nmp}(I_0)C_{nmp}(\alpha)\right] \tag{54}$$

The terms of J_{2l} are canceled out again for the given solutions of s_{2l}, ι_{2l}, o_{2l}, and ϵ_{2l} through the equality of Eq. (32).

We also linearize $\omega_\oplus h_z$ such that

$$\omega_\oplus h_z = (\mu/a)\omega_e(1 + \delta_{2l} + \delta_{nm})\cos I_0 \tag{55}$$

Subtracting Eq. (55) from Eq. (54), we have

$$\mathcal{C} = -(\mu/2a) + (\mu/a)[-\omega_e(1 + \delta_{2l})\cos I_0 + \Delta c] \tag{56}$$

where Δc is given by

$$\Delta c = (1 - \omega_e \cos I_0)\delta_{nm} + \iota_{nm}\tan I_0 - J_{nm}\left(\frac{R}{a}\right)^n \sum_{p=0}^{n} F_{nmp}(I_0)C_{nmp}(\alpha) \tag{57}$$

By substituting ι_{nm} and δ_{nm} solutions of Eq. (44) and Eq. (46), Δc of Eq. (57) becomes

$$\Delta c = -(1 - \omega_e \cos I_0)\left(\delta^0_{nm} + \iota^0_{nm}\tan I_0\right) - \omega_e \iota^0_{nm}\sin I_0 - J_{nm}\left(\frac{R}{a}\right)^n \sum_{p=0}^{n} \frac{(n-2p)\kappa + m\vartheta}{\tau_{nmp}} F_{nmp}(I_0)C_{nmp}(\alpha) \tag{58}$$

Because the last term of Δc Eq. (58) is $\mathcal{O}(J_{2l}J_{nm})$, the first-order approximation to the Jacobi constant $\mathcal{C}$ is obtained through Eq. (56) by

$$\mathcal{C} = -(\mu/2a)\left[1 + 2\omega_e(1 + \delta_{2l})\cos I_0 + 2\omega_e \iota^0_{nm}\sin I_0 + 2(1 - \omega_e \cos I_0)\left(\delta^0_{nm} + \iota^0_{nm}\tan I_0\right)\right] \tag{59}$$

The azimuthal solution we obtained in Eq. (50) has a secular perturbation in the first term, which arises from the constant offset $\delta^0_{nm} + \iota^0_{nm}\tan I_0$ appearing in the radial solution (47). This does not agree with the fact that secular perturbations do not occur away from resonance as a result of the tesseral potentials.[13] This arises from a choice of mean semimajor axis, and hence there should be a well-defined semimajor axis, which gives no secular term. Equation (59) suggests that if we define our semimajor axis a through the Jacobi constant $\mathcal{C}$ such that

$$a = -(\mu/2\mathcal{C})\left[1 + 2\omega_e(1 + \delta_{2l})\cos I_0 + 2\omega_e \iota^0_{nm}\sin I_0\right] \tag{60}$$

then $\delta^0_{nm} + \iota^0_{nm}\tan I_0 = 0$, which removes the secular term, and hence the δ^0_{nm} constant is explicitly determined by

$$\delta^0_{nm} = J_{nm}\left(\frac{R}{a}\right)^n \sum_{p=0}^{n} \frac{[(n-2p)\cos I_0 - m]F_{nmp}(I_0)}{\tau_{nmp}\cos I_0} C_{nmp}(0) \tag{61}$$

through Eq. (48). Because the terms of ω_e, δ_{2l}, and ι^0_{nm} are also functions of semimajor axis a, the iteration scheme can be used to obtain the semimajor axis a defined in Eq. (60). We therefore use Eq. (60) to define our semimajor axis, which is a natural generalization of its definition in our study of perturbations because of axisymmetric potential[5] in terms of conserved orbital energy.

Tesseral Perturbation on Epicycle Coordinates

Having defined the semimajor axis about which we have expanded, we turn now to summarize the solutions for tesseral perturbations to our four coordinates, Eqs. (44), (45), (47), and (50). The correction terms $(s_{nm}, \iota_{nm}, o_{nm}, \epsilon_{nm})$ from n-deg, m-order tesseral harmonic perturbations have the form

$$s_{nm} = \sum_{p=0}^{n} \Delta r_{nmp} C_{nmp}(\alpha)$$

$$\iota_{nm} = \sum_{p=0}^{n} \Delta I_{nmp}[C_{nmp}(\alpha) - C_{nmp}(0)]$$

$$o_{nm} = \sum_{p=0}^{n} \Delta\Omega_{nmp}[S_{nmp}(\alpha) - S_{nmp}(0)]$$

$$\epsilon_{nm} = \sum_{p=0}^{n} \Delta\lambda_{nmp}[S_{nmp}(\alpha) - S_{nmp}(0)] \tag{62}$$

where the constant perturbation coefficients are given by

$$\frac{\Delta r_{nmp}}{a} = -J_{nm}\left(\frac{R}{a}\right)^n \frac{[(n+1)\tau_{nmp} - 2(n-2p)]F_{nmp}(I_0)}{\tau_{nmp}\left(1 - \tau^2_{nmp}\right)}$$

$$\Delta I_{nmp} = J_{nm}\left(\frac{R}{a}\right)^n \frac{[(n-2p)\cos I_0 - m]F_{nmp}(I_0)}{\tau_{nmp}\sin I_0}$$

$$\Delta\Omega_{nmp} = J_{nm}\left(\frac{R}{a}\right)^n \frac{F'_{nmp}(I_0)}{\tau_{nmp}\sin I_0}$$

$$\Delta L_{nmp} = J_{nm}\left(\frac{R}{a}\right)^n \left\{(n-2p) + \frac{2[(n+1)\tau_{nmp} - 2(n-2p)]}{1 - \tau^2_{nmp}}\right\}\frac{F_{nmp}(I_0)}{\tau^2_{nmp}} \tag{63}$$

In Eqs. (63), as Cook defined,[7] we introduce the along-track variation coefficients ΔL_{nmp} by

$$\Delta L_{nmp} = \Delta\lambda_{nmp} + \Delta\Omega_{nmp}\cos I_0 \tag{64}$$

and remember $\tau_{nmp} = (n-2p)(1+\kappa) + m(\vartheta - \omega_e)$ and $m \neq 0$. The $\Delta\lambda_{nmp}$ coefficients, therefore, can be obtained through Eq. (64) by knowing the $\Delta\Omega_{nmp}$ coefficients. From the definition of C_{nmp} and S_{nmp} functions of Eq. (34), we can find the frequencies of tesseral perturbation are therefore given by

$$n_{nmp} = \tau_{nmp} n_0 \tag{65}$$

where n_0 is the original epicycle frequency ($\alpha = n_0 t$) and p runs from zero to n. For a low-Earth orbiting satellite, which commonly rotates 14–15 revolutions per day ($\omega_e \approx 7 \times 10^{-2}$), we assume $m\omega_e \ll 1$ for moderate values of m, for instance, up to and including fourth order. Then, for such m values we note $\kappa, \vartheta \ll m\omega_e$ because κ and ϑ are $\mathcal{O}(J_2)$. Therefore, if $n - 2p \neq 0$ then the tesseral perturbation frequencies n_{nmp} are dominated by $(n-2p)(1+\kappa)n_0$, which is an integer multiple of the nodal frequency $(1+\kappa)n_0$ and gives short periodic variations to epicycle coordinates.

If $n - 2p = 0$, which arises when the degree n is even, then the frequencies become $n_{nmp} = m(\vartheta - \omega_e)n_0$. In this case the period of the perturbation is an integral fraction of a day. These are known as m-daily periodic perturbations.[13] Using the notation of $p_0 = n/2$ in Eqs. (63), the m-daily terms are given by

$$\frac{s_{nm}}{a} = -(n+1)J_{nm}\left(\frac{R}{a}\right)^n F_{nmp_0}(I_0)C_{nmp_0}(\alpha)$$

$$\iota_{nm} = -J_{nm}\left(\frac{R}{a}\right)^n \frac{F_{nmp_0}(I_0)}{(\vartheta - \omega_e)\sin I_0}\left[C_{nmp_0}(\alpha) - C_{nmp_0}(0)\right]$$

$$o_{nm} = J_{nm}\left(\frac{R}{a}\right)^n \frac{F'_{nmp_0}(I_0)}{m(\vartheta - \omega_e)\sin I_0}\left[S_{nmp_0}(\alpha) - S_{nmp_0}(0)\right]$$

$$\epsilon_{nm} + o_{nm}\cos I_0 = 2(n+1)J_{nm}\left(\frac{R}{a}\right)^n \frac{F_{nmp_0}(I_0)}{m(\vartheta-\omega_e)} \times \left[S_{nmp_0}(\alpha) - S_{nmp_0}(0)\right] \quad (66)$$

Terms of $m^2(\vartheta-\omega_e)^2$ are ignored to obtain the results, and only the radial m-daily variation does not have the $(\vartheta-\omega_e)$ divisor.

The explicit coefficients in the along-track variation of ΔL_{nmp} through $J_{4,4}$ are

$$\Delta L_{2,2,1} = \frac{9}{2}J_{2,2}\left(\frac{R}{a}\right)^2 \frac{\sin^2 I_0}{\vartheta-\omega_e}$$

$$\Delta L_{4,1,2} = -\frac{75}{8}J_{4,1}\left(\frac{R}{a}\right)^4 \frac{\left(4-7\sin^2 I_0\right)\sin I_0\cos I_0}{\vartheta-\omega_e}$$

$$\Delta L_{4,2,2} = -\frac{225}{16}J_{4,2}\left(\frac{R}{a}\right)^4 \frac{\left(6-7\sin^2 I_0\right)\sin^2 I_0}{\vartheta-\omega_e}$$

$$\Delta L_{4,3,2} = \frac{525}{4}J_{4,3}\left(\frac{R}{a}\right)^4 \frac{\sin^3 I_0\cos I_0}{\vartheta-\omega_e}$$

$$\Delta L_{4,4,2} = \frac{1575}{16}J_{4,4}\left(\frac{R}{a}\right)^4 \frac{\sin^4 I_0}{\vartheta-\omega_e} \quad (67)$$

These, as we expect, agree with Cook's results.[7] Because all m-daily periodic terms have a $(\vartheta-\omega_e)$ divisor, the amplitude of the periodic variations can be one order larger than that of short periodic perturbations.

As a matter of interest, let us consider the coupling effect between $\Delta L_{2,2,1}$ and $\Delta L_{4,2,2}$ as both terms have a half-day period. We investigate whether the $\Delta L_{2,2,1}$ and $\Delta L_{4,2,2}$ coupling variation becomes smaller in peak amplitude than $\Delta L_{2,2,1}$ alone for some specific range of inclination angles. By computing the peak amplitude of $|\Delta L_{2,2,1}\sin 2(\Omega-\theta_g-\psi_{2,2}) + \Delta L_{4,2,2}\sin 2(\Omega-\theta_g-\psi_{4,2})|$ and knowing $\cos 2(\psi_{4,2}-\psi_{2,2}) < 0$ for the Earth's potential, we can find $\sin I_0$ to satisfy

$$\frac{6}{7} \le \sin^2 I_0 \le \frac{6}{7} - \frac{16}{175}\frac{J_{2,2}}{J_{4,2}}\left(\frac{R}{a}\right)^{-2}\cos 2(\psi_{4,2}-\psi_{2,2}) \quad (68)$$

to make the peak amplitude of $|\Delta L_{2,2,1}\sin 2(\Omega-\theta_g-\psi_{2,2}) + \Delta L_{4,2,2}\sin 2(\Omega-\theta_g-\psi_{4,2})|$ smaller or equal to $|\Delta L_{2,2,1}|$. This corresponds to 67.8 deg $\le I_0 \le$ 71.4 deg or 108.6 deg $\le I_0 \le$ 112.2 deg, when the semimajor axis a is 7178 km (we assume 7178 km semimajor axis throughout this section). It may also be interesting to investigate whether the fourth-degree m-daily perturbation can be larger than the second-degree variation of $\Delta L_{2,2,1}$ for some specific inclination angles. By solving $|\Delta L_{2,2,1}| \le |\Delta L_{4,2,2}|$, this happens when

$$\sin^2 I_0 \le \frac{6}{7} - \frac{8}{175}\frac{J_{2,2}}{J_{4,2}}\left(\frac{R}{a}\right)^{-2} \quad (69)$$

which implies $I_0 \le$ 28.3 deg or 151.7 deg $\le I_0$. The right-hand side of Eq. (69) has to be greater than or equal to zero for solutions to exist. To make the right-hand side of Eq. (69) nonnegative, the semimajor axis a has to satisfy

$$\frac{a}{R} \le \sqrt{\frac{75}{4}\frac{J_{4,2}}{J_{2,2}}} \quad (70)$$

which provides an upper limit to a of approximately 8352.6 km. Hence if the semimajor axis is larger than this value, whatever the inclination angle is, the $J_{4,2}$ m-daily variation amplitude cannot be larger than that of $J_{2,2}$. For the $J_{4,1}$ case this situation can also arise if the inclination angle satisfies

$$|\tan I_0| \le -w + \sqrt[3]{v+\sqrt{v^2+u^3}} + \sqrt[3]{v-\sqrt{v^2+u^3}} \quad (71)$$

where

$$w = \frac{25}{12}\frac{J_{4,1}}{J_{2,2}}\left(\frac{R}{a}\right)^2, \qquad v = \frac{5}{2}w - w^3, \qquad u = \frac{1}{3} - w^2 \quad (72)$$

This gives $I_0 \le$ 38.5 deg or 141.5 deg $\le I_0$ to make the effect of $J_{4,1}$ larger than that of $J_{2,2}$. Unlike the $J_{4,2}$ case, the m-daily periodic variation from $J_{4,1}$ can be larger than the $J_{2,2}$ variation for some inclination angles without any semimajor axis limitations.

Such a particular case will not happen for both $J_{4,3}$ and $J_{4,4}$ cases because the conditions to make $|\Delta L_{2,2,1}| \le |\Delta L_{4,3,2}|$ and $|\Delta L_{2,2,1}| \le |\Delta L_{4,4,2}|$ are obtained by

$$|\sin 2I_0| \ge \frac{12}{175}\frac{J_{2,2}}{J_{4,3}}\left(\frac{R}{a}\right)^{-2}, \qquad \sin^2 I_0 \ge \frac{8}{175}\frac{J_{2,2}}{J_{4,4}}\left(\frac{R}{a}\right)^{-2} \quad (73)$$

however, the right-hand sides of both inequalities are larger than one for the Earth's potential. All of the m-daily periodic terms shown in Eq. (67) vanish for an equatorial orbit, e.g., $I_0 = 0$.

Our radial and azimuthal solutions, given in Eqs. (47) and (50), both appear to have $1-\tau_{nmp}^2$ divisors. Therefore if $1-\tau_{nmp}^2 = \mathcal{O}(m\omega_e)$, we can have $\mathcal{O}(J_{nm}/m\omega_e)$ short-periodic variations in radial and azimuthal coordinates. If degree n is odd and we consider two values $p_\pm = (n\mp 1)/2$, then we have

$$\tau_{nmp_\pm} = \pm(1+\kappa) + m(\vartheta-\omega_e) \quad (74)$$

and if order m is small enough, then we can approximate

$$1 - \left(\tau_{nmp_\pm}\right)^2 \approx \mp 2[m(\vartheta-\omega_e) \pm \kappa] \quad (75)$$

and obtain the terms of interest as follows:

$$\frac{s_{nm}}{a} = \pm\chi_{nmp_\pm}C_{nmp_\pm}(\alpha)$$

$$\epsilon_{nm} = \mp 2\chi_{nmp_\pm}\left[S_{nmp_\pm}(\alpha) - S_{nmp_\pm}(0)\right] \quad (76)$$

where

$$\chi_{nmp_\pm} = \frac{1}{2}(n-1)J_{nm}\left(\frac{R}{a}\right)^n \frac{F_{nmp_\pm}(I_0)}{m(\vartheta-\omega_e)\pm\kappa} \quad (77)$$

The explicit descriptions of $\chi_{nmp_\pm}$ for the third-order tesseral harmonics are given by

$$\chi_{3,1,p_\pm} = \frac{3}{16}J_{3,1}\left(\frac{R}{a}\right)^3 \frac{5\sin^2 I_0(1\pm 3\cos I_0) - 4(1\pm\cos I_0)}{\vartheta-\omega_e\pm\kappa}$$

$$\chi_{3,2,p_\pm} = \pm\frac{15}{8}J_{3,2}\left(\frac{R}{a}\right)^3 \frac{\sin I_0\left(1\mp 2\cos I_0 - 3\cos^2 I_0\right)}{2(\vartheta-\omega_e)\pm\kappa}$$

$$\chi_{3,3,p_\pm} = \frac{45}{8}J_{3,3}\left(\frac{R}{a}\right)^3 \frac{\sin^2 I_0(1\pm\cos I_0)}{3(\vartheta-\omega_e)\pm\kappa} \quad (78)$$

where $p_+ = 1$ and $p_- = 2$. We show that for the odd-degree tesseral harmonics, if the value of m is moderately small, the short-periodic perturbations have $m(\vartheta-\omega_e)\pm\kappa$ divisor and have frequencies of $(1+\kappa)n_0 \pm m(\vartheta-\omega_e)n_0$. This is approximately the epicycle orbital frequency n_0 so that these terms might introduce m-daily periodic variations in both the epicycle amplitude and phase at perigee passage because of the coupling effect with the original epicycle term. If we combine the epicycle term into our radial solution of Eq. (76), then we have

$$s_{nm} = -A\cos(\alpha-\alpha_P) \pm a\chi_{nmp_\pm}C_{nmp_\pm} \quad (79)$$

By introducing the notations of $\hat{A}$ and $\hat{\alpha}_P$ for the perturbed epicycle amplitude and phase at perigee passage,

$$\hat{A}\cos\hat{\alpha}_P = A\cos(\alpha_p + \kappa\alpha) - a\chi_{nmp_\pm}\begin{Bmatrix}\pm\cos\\ \pm\sin\end{Bmatrix}_{(n-m)\text{ odd}}^{(n-m)\text{ even}} m(\Omega-\theta_g-\psi_{nm})$$

$$\hat{A}\sin\hat{\alpha}_P = A\sin(\alpha_p + \kappa\alpha)$$

$$+ a\chi_{nmp\pm}\begin{Bmatrix}\sin\\ -\cos\end{Bmatrix}^{(n-m)\text{ even}}_{(n-m)\text{ odd}} m(\Omega - \theta_g - \psi_{nm}) \tag{80}$$

where $\Omega = \Omega_0 + \vartheta\alpha$, we can arrange the radial equation (79) such that

$$s_{nm} = -\hat{A}\cos(\alpha + \kappa\alpha - \hat{\alpha}_P) \tag{81}$$

We have shown, through Eq. (80), that the odd-degree tesseral harmonics give m-daily periodic perturbations to our epicycle amplitude and phase at perigee passage.

Simulation Results

Even-Degree Tesseral

The simulation we shall present compares the epicycle description of the orbit using the second harmonic of potential, namely, the disturbing potential V is given by

$$V = (\mu/r)\big[J_2(R/r)^2P_2(\cos\theta) - J_{2,2}(R/r)^2P_2^2(\cos\theta)\cos 2(\psi - \psi_{2,2})\big] \tag{82}$$

We ignore $J_{2,1}$ term because it is three order of magnitude smaller than $J_{2,2}$ ($J_{2,1} \approx 1.56\times10^{-9}$, whereas $J_{2,2} \approx 1.82\times10^{-6}$ given by JGM-2 model[13]). J_2 second-order terms are included for this simulation because $\mathcal{O}(J_2^2) = \mathcal{O}(J_{2,2}) = \mathcal{O}(10^{-6})$. The epicycle description of this orbit is summarized by

$$r = a(1+\varrho_2) - A\cos(\alpha - \alpha_P) + \Delta r_2 + s_{2,2}$$

$$I = I_0 + \Delta I_2 + \iota_{2,2}, \qquad \Omega = \Omega_0 + \vartheta_2\alpha + \Delta\Omega_2 + o_{2,2}$$

$$\lambda = (1+\kappa_2)\alpha + (2A/a)[\sin(\alpha - \alpha_P) + \sin\alpha_P] + \Delta\lambda_2 + \epsilon_{2,2} \tag{83}$$

where ϱ_2, ϑ_2, and κ_2 are secular constant coefficients caused by J_2 zonal potential including J_2 second-order corrections, and Δr_2, ΔI_2, $\Delta\Omega_2$, and $\Delta\lambda_2$ represent all of the periodic perturbation terms of $\mathcal{O}(J_2, J_2^2, J_2(A/a), (A/a)^2)$. Explicit expressions of these terms are given in Hashida and Palmer.[5] The tesseral periodic coefficients for $s_{2,2}$, $\iota_{2,2}$, $o_{2,2}$, and $\epsilon_{2,2}$ are shown in the Appendix of this paper. The analytic description is then compared with the output propagated by a second-order Bulirsch–Stoer integrator.[14] This integration method provides high levels of orbital accuracy as well as very short integration times.

We define our starting conditions in terms of the position and velocity of the satellite at some initial epoch $t = 0$, hence at an ascending node $\lambda = 0$. Then the osculating orbital plane is defined as the plane containing the position and velocity vector, and once this plane has been defined we can immediately determine the inclination I_0 and right ascension of the ascending node Ω_0. For the given satellite's initial position and velocity we can compute the Jacobi constant $\mathcal{C}$ without any truncations through Eq. (29). From this we obtain our mean semimajor axis by solving Eq. (60) iteratively. All that remains for the epicycle description of the orbit are the epicycle amplitude A and the epicycle phase at perigee α_P. These appeared as constants of integration in our radial equation. Because everything else is known, the radial position of the satellite then gives a value for $A\cos\alpha_P$, where we have used the fact that $\alpha = 0$ at the initial epoch. Differentiating the equation for r gives the radial velocity and an expression for $A\sin\alpha_P$. These are then easily solved for the remaining unknowns. This completes the set of epicycle parameters that we require.

We have chosen a low Earth orbit with a semimajor axis of 7178 km, which is about 800 km orbital altitude. The numerically integrated orbit and the analytic orbit are both propagated for 360 days (which corresponds to more than 5000 orbits) in order to determine the magnitude of the errors.

In Fig. 1 we have plotted the peak positional error in terms of along, cross, and radial directions over the 360 days propagation as a function of inclination angle. To obtain the result, we have chosen the initial condition to give a very small epicycle amplitude, $A/a \approx \mathcal{O}(10^{-9})$. For this simulation it appears to have a peak error around the inclination of 50 deg. This result shows, however, the dominant along-track peak errors are at most approximately 0.7 km (1×10^{-4} rad for the given value of the semimajor axis) for all inclinations. If we consider 5000-orbit propagation time, the epicycle phase α reaches more than 3×10^4 rad, then this order of along-track error indicates that the error in semimajor axis $\Delta a/a$ is $\mathcal{O}(10^{-8}) \sim \mathcal{O}(10^{-9})$ by assuming $\Delta a/a \approx -(\frac{2}{3})\Delta n_0/n_0 = -(\frac{2}{3})\Delta\alpha/\alpha$. This order of error might come from unmodeled J_2^3 or $J_2J_{2,2}$ terms.

The peak positional error as a function of (normalized) epicycle amplitude is also presented in Fig. 2; here the inclination angle is

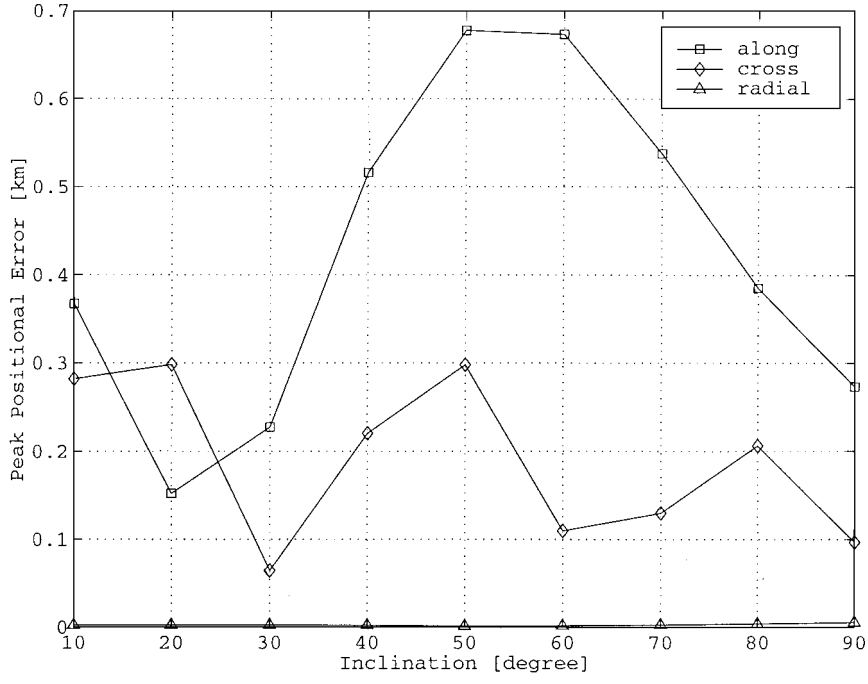

Fig. 1 Peak positional error in along-track, cross-track, and radial direction during 5000 orbits propagation (in kilometers) as a function of inclination angle (in degrees).

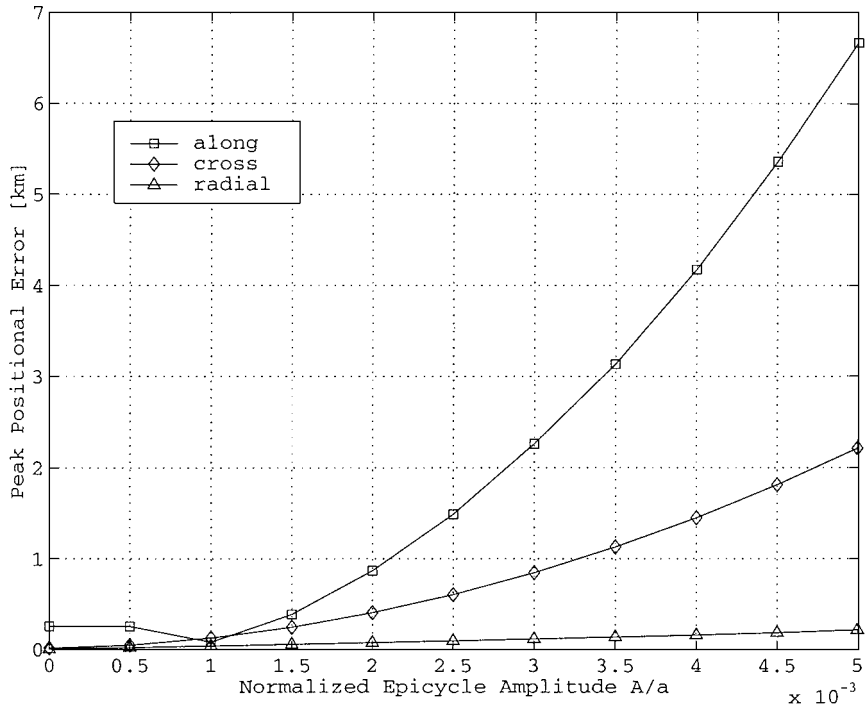

Fig. 2 Peak positional error in along-track, cross-track, and radial direction during 5000 orbits propagation (in kilometers) as a function of normalized epicycle amplitude A/a (or eccentricity). The inclination angle is 98 deg.

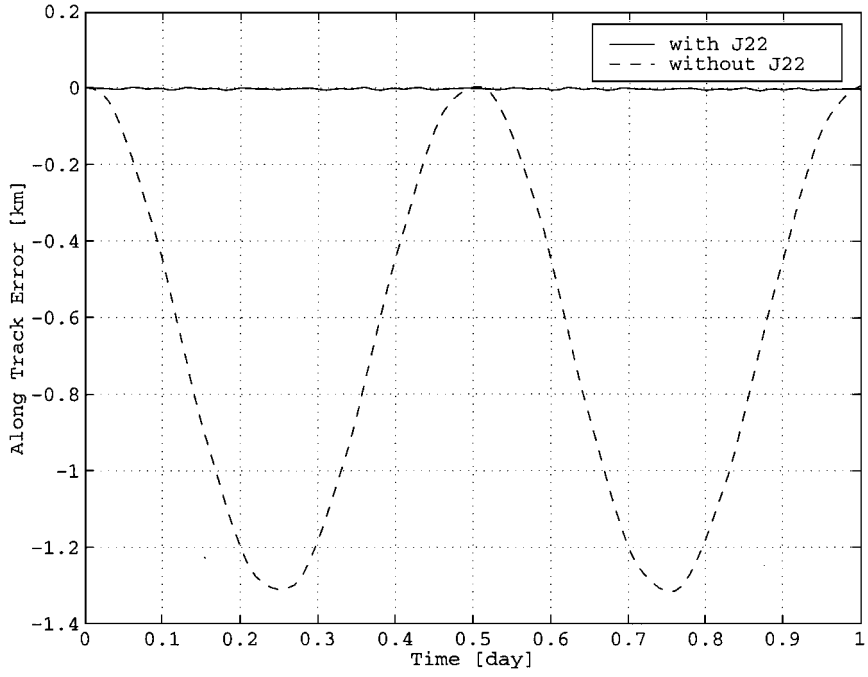

Fig. 3 Error in along-track direction (in kilometers) as a function of propagation time (in days). The inclination angle is 98 deg. The - - - indicates errors without $J_{2,2}$ terms in epicycle formulation.

fixed to be 98 deg to obtain the result. This plot shows that the error increases as the epicycle amplitude becomes larger. The peak along-track error reaches 7 km at $A/a = 5 \times 10^{-3}$ corresponding to the error in semimajor axis of $\Delta a/a \approx 2 \times 10^{-8}$. This is, however, caused by our assumption of $\mathcal{O}(A/a) \approx \mathcal{O}(J_2)$, by which we establish our ordering scheme of perturbation terms.

We have propagated two orbits for one day by our epicycle formulation, one including and the other excluding $J_{2,2}$ terms. We have used zero epicycle amplitude and 98 deg inclination. The along-track propagation errors of the two epicycle orbits with respect to the time are presented in Fig. 3. We have chosen the initial ascending node Ω_0 and sidereal angle θ_0 such that $2(\Omega_0 - \theta_0 - \psi_{2,2}) = \pi/2$. So that the half-daily along-track solution from $J_{2,2}$ is arranged by

$$\epsilon_{2,2} + o_{2,2} \cos I_0 = -\Delta L_{2,2,1}[1 - \cos(2\vartheta_2 - 2\omega_e)] \tag{84}$$

We can clearly see the effect of half-daily periodic perturbation in Fig. 3. The amplitude of this half-daily periodic variation seems to reach almost 1.3 km, leading 1.9×10^{-4} rad variation in the along-track direction while this is, through Eqs. (67), given by

$$|\Delta L_{2,2,1}| = \frac{9}{2} J_{2,2} \left(\frac{R}{a}\right)^2 \frac{\sin^2 I_0}{|\vartheta_2 - \omega_e|} \tag{85}$$

Considering the orbit we are assuming, which is 7178-km semimajor axis and 98-deg inclination that gives $\omega_e \approx 7.0 \times 10^{-2}$, $R/a \approx 8.9 \times 10^{-1}$, and $\sin I_0 \approx 9.9 \times 10^{-1}$, then Eq. (85) indicates

the magnitude of half-daily variation $|\Delta L_{2,2,1}|$ of 9.0×10^{-5}, which gives 1.8×10^{-4} at the peak through Eq. (84). This agrees with the result we have obtained. As we can see in Fig. 3, if the $J_{2,2}$ terms are taken into account in the epicycle formulas, then the propagation error, compared to the reference orbit, becomes significantly smaller.

Odd-Degree Tesseral

We have also performed the simulation to justify our results from the odd- degree tesseral potential. We have chosen the third-degree second-order tesseral $J_{3,2}$ for our simulation, namely, we assume that the disturbing potentail V is

$$V = (\mu/r)\left[J_2(R/r)^2 P_2(\cos\theta) - J_{3,2}(R/r)^3 P_3^2(\cos\theta)\cos 2(\psi - \psi_{3,2})\right] \quad (86)$$

The epicycle formulation of this orbit is similar to Eqs. (83), and all of the $J_{3,2}$ tesseral periodic coefficients are also introduced in the Appendix. As we did in the preceding section, two orbits have been propagated for one day, one including and the other excluding $J_{3,2}$ terms. A 7178-km semimajor axis, zero epicycle amplitude, and 98-deg inclined orbit are used for this simulation. We choose the initial ascending node Ω_0 and sidereal angle θ_0 to satisfy $2(\Omega_0 - \theta_0 - \psi_{3,2}) = \pi/2$. The along-track propagation errors of the

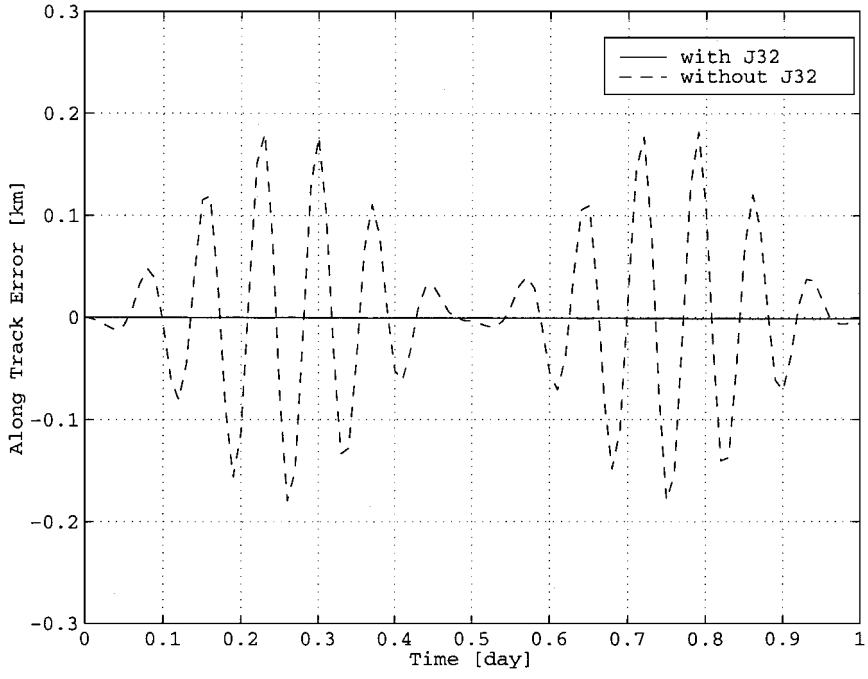

Fig. 4 Error in along-track direction (in kilometers) as a function of propagation time (in days). The inclination angle is 98 deg. The – – – indicates errors without $J_{3,2}$ terms in epicycle formulation.

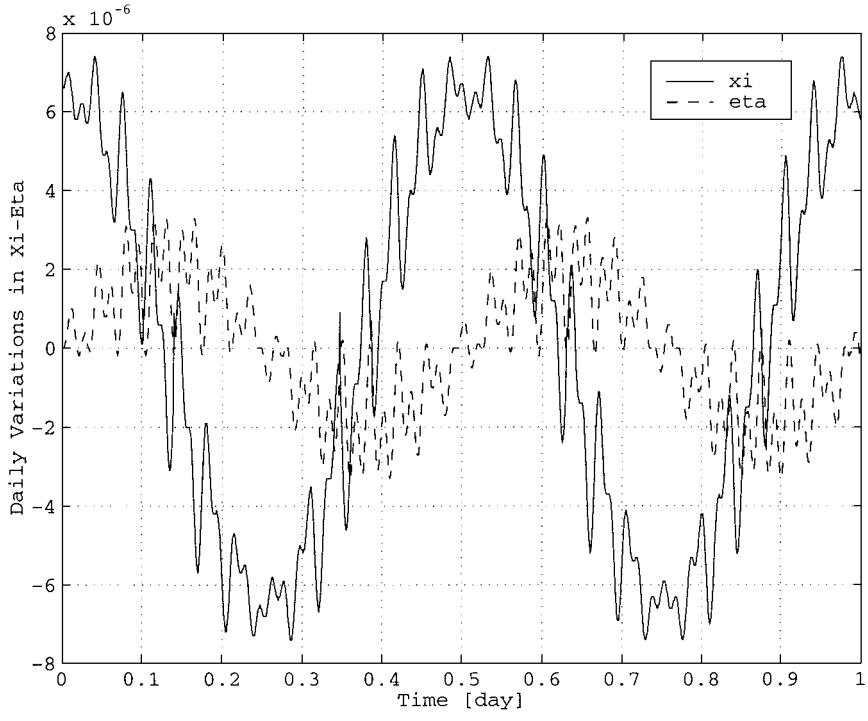

Fig. 5 Variations in $\xi = (\hat{A}/a)\cos\hat{\alpha}_P$ and $\eta = (\hat{A}/a)\sin\hat{\alpha}_P$ from the $J_{3,2}$ terms as a function of propagation time (in days). $\hat{A}$ and $\hat{\alpha}_P$ are osculating epicycle amplitude and phase at perigee passage, respectively.

two orbits with respect to the elapsed time are shown in Fig. 4. We can see the one orbital periodic variation with the one-day periodic envelope in Fig. 4 if $J_{3,2}$ terms are neglected. This is caused by the coupling effect of terms with two frequencies, approximately n_0 and $(1 \pm 2\omega_e)n_0$.

The epicycle amplitude for the given initial condition is $A/a \approx 7.5 \times 10^{-6}$, when $J_{3,2}$ terms are ignored. This orginal epicycle term introduces frequency of n_0 and $\chi_{3,2,1}$ and $\chi_{3,2,2}$ terms in Eqs. (78) have frequencies of $(1+\kappa_2) \pm 2(\vartheta_2 - \omega_e)n_0 \approx (1 \mp 2\omega_e)n_0$. The results show that the peak periodic perturbation can reach about 0.2 km, which corresponds to approximately 2.8×10^{-5} radians in the along-track direction. Because of our choice of Ω_0 and θ_0, the along-track solution of these terms is arranged by

$$\epsilon_{3,2} + o_{3,2}\cos I_0 = \Delta L_{3,2,1}\sin[(1+\kappa_2+2\vartheta_2-2\omega_e)\alpha] - \Delta L_{3,2,2}\sin[(1+\kappa_2-2\vartheta_2+2\omega_e)\alpha] \tag{87}$$

Let us evaluate the magnitude of $\chi_{3,2,p_\pm}$ terms:

$$\left|\chi_{3,2,p_\pm}\right| = \frac{15}{8}J_{3,2}\left(\frac{R}{a}\right)^3\left|\frac{\sin I_0\left(1 \mp 2\cos I_0 - 3\cos^2 I_0\right)}{2(\vartheta_2 - \omega_e) \pm \kappa_2}\right| \tag{88}$$

for the given orbit. Using the values of ω_e, R/a in the preceding section and $J_{3,2} \approx 3.74 \times 10^{-7}$, we have $|\chi_{3,2,1}| \approx 4.3 \times 10^{-6}$ and $|\chi_{3,2,2}| \approx 2.3 \times 10^{-6}$. Therefore, from the along-track variation coefficients in Eqs. (A17) in the Appendix and the along-track epicycle coefficients of $2A/a$, the peak variation of $J_{3,2}$ peridic terms can reach what we have obtained through the simulation. If we include $J_{3,2}$ terms, we obtain significant agreement with the reference obrit.

We have also presented the half-daily periodic variation in our epicycle amplitude and phase at perigee passage as a result of the $J_{3,2}$ tesseral potential. To identfy this variation clearly, we have disabled the J_2 potential, e.g., we pretend $J_2 = 0$ in the disturbing potential V defined in Eq. (86).We have used the initial condition to give the "mean" epicycle amplitude $A/a = 1.1 \times 10^{-6}$ in Eqs. (80) for this simulation. The epicycle orbit without J_2 perturbations is propagated for one day, and the osculating orbital elements are derived at every sampling step. Using the osculating epicycle amplitude $\hat{A}$ and the epicycle phase of perigee passage $\hat{\alpha}_P$, we define two parameters of $\xi := (\hat{A}/a)\cos\hat{\alpha}_P$ and $\eta := (\hat{A}/a)\sin\hat{\alpha}_P$. These two parameters with respect to the time are shown in Fig. 5. We can clearly see the half-daily periodic variations in both ξ and η as we discussed in the preceding section. Because we neglect J_2 term, the variations in ξ and η are $\mathcal{O}(10^{-6}) \sim \mathcal{O}(10^{-5})$ and mainly introduced by $\chi_{3,2,1}$ and $\chi_{3,2,2}$ terms, which have the ω_e divisor.

Conclusions

We have presented the solution for the motion of a satellite in a near-circular orbit perturbed by the tesseral potential. We formulate the perturbed orbit by the use of epicycle motion for the radial and azimuthal solutions and another two coordinates: instantaneous (or osculating) inclination and ascending node. Our formulation is valid for orbital eccentricities of order comparable to J_2 or smaller.

This representation requires four coordinates to locate the satellite, but greatly simplifies the description of the motion and gives a simple geometric interpretation with concise form. We have given the tesseral perturbation terms that appear in these four coordinates up to an arbitrary degree and order of tesseral potential without any eccentricity divisor.

We have shown even-degree tesserals give m-daily periodic perturbations to the four epicycle coordinates and odd-degree tesserals lead to m-daily periodic perturbations to the epicycle amplitude and phase at perigee passage. We have found that the amplitude of the fourth-degree m-daily perturbations can become larger than that of the second-degree tesseral $J_{2,2}$ for some specific orbits and investigated the conditions for this on both semimajor axis and inclination.

We have compared the predictions of these analytic equations with numerical simulations including the effects of J_2 and $J_{2,2}$, $J_{3,2}$. We have shown that the errors in the semimajor axis of the satellite are of order $\mathcal{O}(10^{-9}) \sim \mathcal{O}(10^{-8})$, which is to be expected by neglecting terms such as J_2^3 or $J_2 J_{2,2}$. We have shown the effect of half-daily periodic variations, which can induce about a kilometer along-track variation for a low Earth-orbiting satellite caused by the $J_{2,2}$ potential. We presented the half-daily perturbations in our epicycle amplitude and phase at pergee passage caused by the odd tesseral $J_{3,2}$ potential.

We have demonstrated that our analytical formulation including tesseral terms provides only subkilometer propagation errors compared with the numerically integrated orbit after 5000 orbits propagation for a low-Earth near-circular orbit.

Appendix: Jacobi Constant and Epicycle Coefficients

Jacobi Constant

We multiply $\dot{\theta}$ through the second of Eqs. (7) to obtain

$$r\dot{\theta}\frac{\mathrm{d}}{\mathrm{d}t}(r\dot{\theta}) + r\dot{r}\dot{\theta}^2 - r^2\dot{\varphi}^2\dot{\theta}\sin\theta\cos\theta = -\frac{\partial V}{\partial\theta}\dot{\theta} \tag{A1}$$

Similarly by multiplying $\dot{\psi}$ through the third of Eqs. (7) and arranging it, we have

$$r\dot{\psi}\sin\theta\frac{\mathrm{d}}{\mathrm{d}t}(r\dot{\psi}\sin\theta) - r\omega_\oplus\sin\theta\frac{\mathrm{d}}{\mathrm{d}t}(r\omega_\oplus\sin\theta) + r\dot{r}\dot{\varphi}^2\sin^2\theta + r^2\dot{\varphi}^2\dot{\theta}\sin\theta\cos\theta = -\frac{\partial V}{\partial\psi}\dot{\psi} \tag{A2}$$

where we rewrite $\theta_g = \theta_0 + \omega_\oplus t$ and $\omega_\oplus$ is the Earth's sidereal rotation rate. We shall also note that $\partial V/\partial\varphi = \partial V/\partial\psi$. Remember ψ is defined by $\psi = \varphi - \theta_g$ through Eq. (9). By using ψ instead of φ, we regard $V(r, \theta, \varphi - \theta_g)$ as $V(r, \theta, \psi)$, which is introduced in Eq. (10). If we multiply $\dot{r}$ through the first of Eqs. (7) and substitute Eqs. (A1) and (A2) to eliminate $r\dot{r}(\dot{\theta}^2 + \dot{\varphi}^2\sin^2\theta)$ term, we have

$$\dot{r}\ddot{r} + r\dot{\theta}\frac{\mathrm{d}}{\mathrm{d}t}(r\dot{\theta}) + r\dot{\psi}\sin\theta\frac{\mathrm{d}}{\mathrm{d}t}(r\dot{\psi}\sin\theta) - r\omega_\oplus\sin\theta\frac{\mathrm{d}}{\mathrm{d}t}(r\omega_\oplus\sin\theta) + \frac{\mu}{r^2}\dot{r} + \dot{V} = 0 \tag{A3}$$

where

$$\dot{V} = \frac{\partial V}{\partial r}\dot{r} + \frac{\partial V}{\partial\theta}\dot{\theta} + \frac{\partial V}{\partial\psi}\dot{\psi} \tag{A4}$$

because $\partial V/\partial t = 0$ in (r, θ, ψ) rotating coordinate. We then integrate Eq. (A3) to obtain Eq. (28).

Epicycle Zonal J_{2l} Coefficients[5]

J_{2l} secular coefficients are

$$\varrho = (2l-1)J_{2l}\left(\frac{R}{a}\right)^{2l}L_{2l}^0$$

$$\vartheta = -2J_{2l}\left(\frac{R}{a}\right)^{2l}\frac{\cot I_0}{\sin I_0}\sum_{k=1}^{l}2kL_{2l}^{2k}$$

$$\kappa = -\vartheta_{2l}\cos I_0 - (4l-1)J_{2l}\left(\frac{R}{a}\right)^{2l}L_{2l}^0 \tag{A5}$$

where

$$L_{2l}^{2k} = \frac{(2l-2k)!}{(2l+2k)!}P_{2l}^{2k}(0)P_{2l}^{2k}(\cos I_0) \tag{A6}$$

J_{2l} periodic coefficients are

$$\Delta r_{2l}^k = 2(2l-1)J_{2l}\left(\frac{R}{a}\right)^{2l}\left[\frac{(-1)^k}{1-(2k)^2}\right]L_{2l}^{2k}a$$

$$\Delta I_{2l}^k = 2J_{2l}\left(\frac{R}{a}\right)^{2l}(-1)^k\cot I_0 L_{2l}^{2k}$$

$$\Delta\Omega_{2l}^k = -2J_{2l}\left(\frac{R}{a}\right)^{2l}(-1)^k\frac{\cot I_0}{\sin I_0}\left(L_{2l}^{2k} + 2\sum_{j=k+1}^{l}\frac{2j}{2k}L_{2l}^{2j}\right)$$

$$\Delta\lambda_{2l}^k = -\Delta\Omega_{2l}^k\cos I_0 - 2J_{2l}\left(\frac{R}{a}\right)^{2l}\frac{(-1)^k}{2k}\left[1 + \frac{2(2l-1)}{1-(2k)^2}\right]L_{2l}^{2k} \tag{A7}$$

Epicycle Tesseral $J_{2,2}$ Coefficients

We introduce the notation of

$$\sigma_{+2} = 2(\vartheta - \omega_e + \kappa), \qquad \sigma_{-2} = 2(\vartheta - \omega_e - \kappa) \tag{A8}$$

and $\sigma_{\pm 2}^2$ are ignored to obtain the following coefficients.

$J_{2,2}$ radial coefficients:

$$\Delta r_{2,2,0} = \tfrac{1}{4} J_{2,2}(R/a)^2 a\left(1 - \tfrac{1}{3}\sigma_{+2}\right)(1 + \cos I_0)^2$$

$$\Delta r_{2,2,1} = -\tfrac{9}{2} J_{2,2}(R/a)^2 a \sin^2 I_0$$

$$\Delta r_{2,2,2} = \tfrac{1}{4} J_{2,2}(R/a)^2 a\left(1 + \tfrac{1}{3}\sigma_{-2}\right)(1 - \cos I_0)^2 \tag{A9}$$

$J_{2,2}$ inclination coefficients:

$$\Delta I_{2,2,0} = -\tfrac{3}{4} J_{2,2}(R/a)^2\left(1 - \tfrac{1}{2}\sigma_{+2}\right)\sin I_0(1 + \cos I_0)$$

$$\Delta I_{2,2,1} = -\tfrac{3}{2} J_{2,2}(R/a)^2[\sin I_0/(\vartheta - \omega_e)]$$

$$\Delta I_{2,2,2} = \tfrac{3}{4} J_{2,2}(R/a)^2\left(1 + \tfrac{1}{2}\sigma_{-2}\right)\sin I_0(1 - \cos I_0) \tag{A10}$$

$J_{2,2}$ ascending node coefficients:

$$\Delta\Omega_{2,2,0} = -\tfrac{3}{4} J_{2,2}(R/a)^2\left(1 - \tfrac{1}{2}\sigma_2\right)(1 + \cos I_0)$$

$$\Delta\Omega_{2,2,1} = \tfrac{3}{2} J_{2,2}(R/a)^2[\cos I_0/(\vartheta - \omega_e)]$$

$$\Delta\Omega_{2,2,2} = -\tfrac{3}{4} J_{2,2}(R/a)^2\left(1 + \tfrac{1}{2}\sigma_{-2}\right)(1 - \cos I_0) \tag{A11}$$

$J_{2,2}$ argument of latitude coefficients (We denote $\Delta L_{2,2,p} := \Delta\lambda_{2,2,p} + \Delta\Omega_{2,2,p}\cos I_0$.):

$$\Delta L_{2,2,0} = \tfrac{1}{8} J_{2,2}(R/a)^2\left(1 - \tfrac{4}{3}\sigma_{+2}\right)(1 + \cos I_0)^2$$

$$\Delta L_{2,2,1} = \tfrac{9}{2} J_{2,2}(R/a)^2\left[\sin^2 I_0 \big/ (\vartheta - \omega_e)\right]$$

$$\Delta L_{2,2,2} = -\tfrac{1}{8} J_{2,2}(R/a)^2\left(1 + \tfrac{4}{3}\sigma_{-2}\right)(1 - \cos I_0)^2 \tag{A12}$$

Epicycle Tesseral $J_{3,2}$ Coefficients

We introduce the notation of

$$\sigma_{+1} = 2(\vartheta - \omega_e) + \kappa, \qquad \sigma_{-1} = 2(\vartheta - \omega_e) - \kappa$$

$$\sigma_{+3} = 2(\vartheta - \omega_e) + 3\kappa, \qquad \sigma_{-3} = 2(\vartheta - \omega_e) - 3\kappa \tag{A13}$$

and $\sigma_{\pm 1}^2$, $\sigma_{\pm 3}^2$ are ignored to obtain the following coefficients.

$J_{3,2}$ radial coefficients:

$$\Delta r_{3,2,0} = \tfrac{15}{32} J_{3,2}(R/a)^3 a\left(1 - \tfrac{5}{12}\sigma_{+3}\right)\sin I_0(1 + \cos I_0)^2$$

$$\Delta r_{3,2,1} = a\chi_{3,2,1}, \qquad \Delta r_{3,2,2} = a\chi_{3,2,2}$$

$$\Delta r_{3,2,3} = -\tfrac{15}{32} J_{3,2}(R/a)^3 a\left(1 + \tfrac{5}{12}\sigma_{-3}\right)\sin I_0(1 - \cos I_0)^2 \tag{A14}$$

$J_{3,2}$ inclination coefficients:

$$\Delta I_{3,2,0} = -\tfrac{5}{8} J_{3,2}(R/a)^3\left(1 - \tfrac{1}{3}\sigma_{+3}\right)(2 - 3\cos I_0)(1 + \cos I_0)^2$$

$$\Delta I_{3,2,1} = -\tfrac{15}{8} J_{3,2}(R/a)^3(1 - \sigma_{+1})(2 - \cos I_0)$$
$$\times\left(1 - 2\cos I_0 - 3\cos^2 I_0\right)$$

$$\Delta I_{3,2,2} = -\tfrac{15}{8} J_{3,2}(R/a)^3(1 + \sigma_{-1})(2 + \cos I_0)$$
$$\times\left(1 + 2\cos I_0 - 3\cos^2 I_0\right)$$

$$\Delta I_{3,2,3} = -\tfrac{5}{8} J_{3,2}(R/a)^3\left(1 + \tfrac{1}{3}\sigma_{-3}\right)(2 + 3\cos I_0)(1 - \cos I_0)^2 \tag{A15}$$

$J_{3,2}$ ascending node coefficients:

$$\Delta\Omega_{3,2,0} = -\frac{5}{8} J_{3,2}\left(\frac{R}{a}\right)^3\left(1 - \frac{1}{3}\sigma_{+3}\right)$$
$$\times \frac{1 + \cos I_0}{\sin I_0}\left(2 - \cos I_0 - 3\cos^2 I_0\right)$$

$$\Delta\Omega_{3,2,1} = \frac{15}{8} J_{3,2}\left(\frac{R}{a}\right)^3(1 - \sigma_{+1})$$
$$\times \frac{1 + \cos I_0}{\sin I_0}\left(2 + 5\cos I_0 - 9\cos^2 I_0\right)$$

$$\Delta\Omega_{3,2,2} = -\frac{15}{8} J_{3,2}\left(\frac{R}{a}\right)^3(1 + \sigma_{-1})$$
$$\times \frac{1 - \cos I_0}{\sin I_0}\left(2 - 5\cos I_0 - 9\cos^2 I_0\right)$$

$$\Delta\Omega_{3,2,3} = \frac{5}{8} J_{3,2}\left(\frac{R}{a}\right)^3\left(1 + \frac{1}{3}\sigma_{-3}\right)$$
$$\times \frac{1 - \cos I_0}{\sin I_0}\left(2 + \cos I_0 - 3\cos^2 I_0\right) \tag{A16}$$

$J_{3,2}$ argument of latitude coefficients (We denote $\Delta L_{3,2,p} := \Delta\lambda_{3,2,p} + \Delta\Omega_{3,2,p}\cos I_0$.):

$$\Delta L_{3,2,0} = \tfrac{5}{16} J_{3,2}(R/a)^3\left(1 - \tfrac{7}{12}\sigma_{+3}\right)\sin I_0(1 + \cos I_0)^2$$

$$\Delta L_{3,2,1} = \tfrac{15}{8} J_{3,2}(R/a)^3(1 - 2\sigma_{+1})\sin I_0$$
$$\times\left(1 - 2\cos I_0 - 3\cos^2 I_0\right) - 2\chi_{3,2,1}$$

$$\Delta L_{3,2,2} = \tfrac{15}{8} J_{3,2}(R/a)^3(1 + 2\sigma_{-1})\sin I_0$$
$$\times\left(1 + 2\cos I_0 - 3\cos^2 I_0\right) - 2\chi_{3,2,2}$$

$$\Delta L_{3,2,3} = \tfrac{5}{16} J_{3,2}(R/a)^3\left(1 + \tfrac{7}{12}\sigma_{-3}\right)\sin I_0(1 - \cos I_0)^2 \tag{A17}$$

References

[1] Kozai, Y., "The Motion of a Close Earth Satellite," *Astronomical Journal*, Vol. 64, No. 2174, 1959, pp. 367–377.

[2] Brouwer, D., "Solution of the Problem of Artificial Satellite Theory Without Drag," *Astronomical Journal*, Vol. 64, No. 1274, 1959, pp. 378–397.

[3] Merson, R. H., "The Motion of Satellite in an Axi-Symmetric Gravitational Field," *Geophysics Journal*, Vol. 4, 1961, pp. 17–52.

[4] Cook, G. E., "Perturbations of Near-Circular Orbits by the Earth's Gravitational Potential," *Planetary and Space Science*, Vol. 14, 1966, pp. 433–444.

[5] Hashida, Y., and Palmer, P. L., "Epicyclic Motion of Satellites About an Oblate Planet," *Journal of Guidance, Control, and Dynamics*, Vol. 24, No. 3, 2001, pp. 586–596.

[6] Musen, P., "On the Motion of a Satellite in an Asymmetrical Gravitational Field," *Journal of Geophysical Research*, Vol. 65, No. 9, 1960, pp. 2783–2792.

[7] Cook, G. E., "Perturbations of Satellite Orbits by Tesseral Harmonics in the Earth's Gravitational Potential," *Planetary and Space Science*, Vol. 11, 1963, pp. 797–815.

[8] Kaula, W. M., *Theory of Satellite Geodesy*, Blaisdell, Waltham, MA, 1966, pp. 31–41.

[9] Palmer, P. L., *Stability of Collisionless Stellar Systems*, Kluwer Academic, Norwell, MA, 1994, pp. 316, 317.

[10] Blitzer, L., Boughton, E. M., Kang, G., and Page, R. M., "Effect of Ellipticity of the Equator on 24-Hour Nearly Circular Satellite Orbits," *Journal of Geophysical Research*, Vol. 67, No. 1, 1962, pp. 329–335.

[11] Gedeon, G. S., "Tesseral Resonance Effects on Satellite Orbits," *Celestial Mechanics*, Vol. 1, 1969, pp. 167–189.

[12] Frauenholz, R. B., Bhat, R. S., Shapiro, B. E., and Leavitt, R. K., "Analysis of the TOPEX/Poseidon Operational Orbit: Observed Variations and Why," *Journal of Spacecraft and Rockets*, Vol. 35, No. 2, 1998, pp. 212–224.

[13] Vallado, D. A., *Fundamentals of Astrodynamics and Applications*, McGraw–Hill, New York, 1997, pp. 588–590, 597–603.

[14] Palmer, P. L., Aarseth, S. J., Mikkola, S., and Hashida, Y., "High Precision Integration Methods for Orbit Modelling," *Journal of Astronautical Sciences*, Vol. 46, No. 4, 1998, pp. 329–342.